



MAXIMUM POWER QUALITY TRACKING OF ARTIFICIAL NEURAL NETWORK CONTROLLER-BASED DOUBLE FED INDUCTION GENERATOR FOR WIND ENERGY CONVERSION SYSTEM

RAJENDRAN ELUMALAI¹

Keywords: Artificial neural network (ANN); Doubly fed induction generator (DFIG); Wind energy conversion systems (WECSs); Distribution static compensator(DSTATCOM); Total harmonics distortion (THD); Power quality (PQ).

Renewable energy sources are playing a crucial role in satisfying the upcoming energy source needs for the world. The current power system is power electronics converter based, with several non-linear loads and spotted generations of renewable energy sources, resulting in many power quality issues. Most existing research analyzed MATLAB simulations and presented a high Total Harmonics Distortion (THD) level. This research work proposed an artificial neural network (ANN) control technique for a doubly fed induction generator (DFIG) based wind energy conversion systems (WECSs). To decrease chattering phenomena during the excitation arrangement, an advanced controller works for adaptive modification of the irregular power gain, even preserving the strength of the closed-loop scheme. The proposed PI controller one step forward improves reliability and tracks maximum voltage from the pulse width modulation rectifier. At primary, the modeling of the DFIG was presented. Then, using the proposed ANN controller, the rotor magnitude was tuned to recognize vector control of active and reactive power. The converter intends to activate at unity power factor and provide input currents with adequate harmonic content. The interface between the power's electronic converter and the DFIG pulls out the most real power potential. The proposed prototype hardware model and simulation results are verified.

1. INTRODUCTION

Wind turbines convert wind energy into mechanical energy, fed into an induction generator to generate electrical power. The crucial stage is a permanent speed wind turbine using a squirrel cage induction generator (SCIG) and capacitor banks. It's low-cost and simple. Currently, variable speed induction generators have been employed to attain the necessary speed by utilizing power electronic converters. DFIG has been extensively utilized in wind energy conversion systems (WECSs). Its advantages are the changeable speed operation, low price, and superior efficiency. The character of DFIG with manufacturers has seen a solid turn down more than the last few years, first and foremost due to complexity within adhering to scientific needs stated in most modern grid codes. The sub-synchronous approach will allow wind power consumption at a worse wind speed. During the sub-synchronous approach, the rotor will acquire the power beginning ac mains, running as a motor. The super-synchronous approach will run beyond the synchronous speed, and this method is used to feed the Slip power intensity on the ac main supply. With the direct connection of stator terminals towards the grid, the DFIG process can be compromised, going on the supply voltage draw [1]. DFIG is commonly utilized in wind energy conversion systems (WECSs), producing quality power, such as unpredictable speed operation, low expenditure, and high efficiency [2]. The confusion in voltage reports changes the consistency and the worth of power feed near the grid system, including voltage dips [3], voltage distortions [4], and voltage unbalances [5]. The wind power systems typically hold up a 3 % unbalance for voltages less than 220 kV. Moreover, 1.5 % with 2 % unbalance restrictions is clear for WECSs functioning by voltages away from 220 and 400 kV, respectively. Unbalanced voltages and considerable negative sequence currents become noticeable in stator and rotor circuits due to uneven heating of DFIG windings, a higher risk of over currents [6]. The voltages disturb arising suitable to repeat unsymmetrical faults during the power

system, particularly fear manufacturers and researchers who are identical. As per rules, the regulations favor grid integration [7]. The considered system control is tested and authorized during statistical simulation. The obtained consequences demonstrate the efficiency of the control strategy, which is most important to the greatest performance, and hardware analysis is not done [8]. The stator current injects keen on the grid short total harmonic distortion (THD) identical to 3.7 % convinced in the IEEE harmonic standard 519. The usual implementation is a minor switching frequency of the converter [9]. The performance is taken in dSPACE1104, a particular board card manager and an acquisition interface. The obtained results are usually used to control nearby fine performance in steady and transient states through low THD in the stator injected current to the grid [10]. Neuro-fuzzy control and Type2 fuzzy logic controller performances are investigated, compared, and obtained starting with the Model Reference Adaptive Controller on behalf of power control. The results verify MATLAB/Simulink only, and hardware analysis was not done [11]. The parameter is achieved under the synchronous speed (hypo-synchronous mode). The implementation is understood via the dSPACE1104 single board control and acquisition interface. The result of the typical control is present fine performance in steady and transient states, not in dynamic states [12]. Using the considered Adaptive Fast Terminal Synergetic Controller, with new various future, allowed the dc-dc step-down converter's state variables to track the preferred reference voltage in being there of disturbances starting every initial condition only and not transient condition [13].

DFIG and wind turbines coupled near capacitive series compensated transmission lines are flat to show oscillatory behavior. Moreover, it proves strong for every line impedance series compensation level; it does not require real-time information concerning the grid to which the wind turbine is connected or its parameters [14]. The optimal control approach depends on the linear quadratic regulator (LQR) algorithm. It provides quick meetings and fewer mathematical difficulties. The method evaluates by

¹SKP Engineering College, Tiruvannamalai, Tamil Nadu, India. E-mail: rajendran_electro@skpec.in.

comparing results and obtaining the LQR controller through realization. The grey wolf optimizer algorithm can be optimized, and proportional integral controllers are used to engage and report severe network disturbances [15]. The improved management strategy of DFIG under operating unbalanced grid voltages with a mixed generalized integrator. The hysteresis band control is rotor currents and grid currents. To generate switching sequences for the rotor side converter and grid side converter. This method is a hybrid structure of the second and third-order generalized integrators and works for positive and negative sequence computation with the complex problem-solving method. The conventional method has some drawbacks, such as high grid current oscillation due to nonlinear loads, high PI controller processing time, and high grid current THD and high voltage THD [16]. The involvement of the paper is mentioned below:

- To improve the quality of the converter's input line current in the wind energy system.
- To ensure smooth operation and economical utilization of the inverter.
- Enhanced dynamic performances are evaluated using the predictable technique to generate the finest wind energy.

To provide constant supply voltage to the three-phase grid using ANN controller.

2. PROPOSED SYSTEM DESCRIPTION

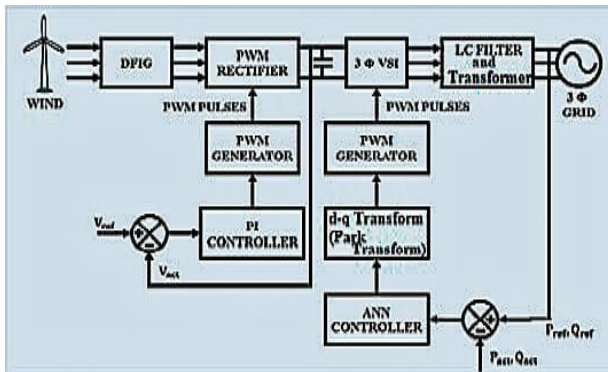


Fig. 1 - Proposed WECS Block Diagram.

The aim of the proposed novel distribution static compensator (DSTATCOM) design to include a 3-phase voltage source inverter is planned for a WECS-based distributed system, as shown in Fig. 1. The DSTATCOM is related to a linear load moreover service grid by way of the parallel connected inductor. The WECS output ac current is converted to direct current using the PWM Rectifier. The output starting from the DFIG-connected WECS is fed to the dc link capacitor C_{dc} , and the compensation current generated to the DSTATCOM is smoothed by the support of a ripple filter, which is coupled parallel through the DSTATCOM. The recompense currents are used to improve power quality. Moreover, it ensures the unity of the power factor of the grid system. The PI regulator is presented for this work, in addition to ensuring a secure voltage level in the dc-link system. Furthermore, the dq theory takes up the current reference for DSTATCOM. Here, the reference current is harmonics-free with the support of an ANN system controller.

2.1 ANALYSIS OF THE DFIG AT A FUNDAMENTAL FREQUENCY

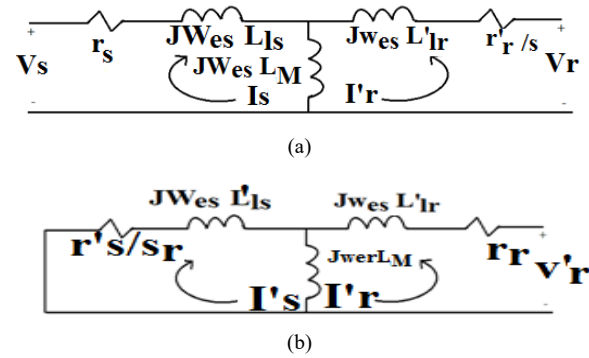


Fig. 2 – DFIG equivalent circuit: (a) stator; (b) rotor.

The common arrangement of the DFIG-supported wind system connected to the power grid is shown in Fig. 1. The Electrical single-line equal phase circuit of the DFIG is shown in Fig. 2, a. A single-line circuit is a predictable, steady-state equivalent model using all parameters referring to the stator. The equation describing the system is given by eq. (1) and (2),

$$V_s = -(r_s + j\omega_e L_s)I_s + j\omega_e L_M I'_r, \quad (1)$$

$$V'_r = r'_s \frac{I'_r}{s} + j\omega_e (L'_r + L_M)I'_r - j\omega_e L_M I_s, \quad (2)$$

where V_s is the stator voltage, V'_r is the rotor voltage, and S defines the virtual velocity linking in the magnetic field created through the currents injected during the stator, as well as the mechanical velocity of the rotor,

$$S = \frac{(\omega_e s - \omega_r)}{\omega_e s} \quad (3)$$

Equations (1) and (2), the stator plus rotor current phasors in the time domains are obtained through

$$i_s = |I_s| \cos(\omega_e t + \phi_s), \quad (4)$$

$$i_r = |I'_r| \cos(s\omega_e t + \phi'_r - \theta_{eff}), \quad (5)$$

where “ i_s ” is the stator current and “ i_r ” is the rotor current.

The slip is analyzed as follows: if the machine is not running, the shaft's mechanical speed is zero ($\omega_r=0$), resulting in a slip value 1 ($s=1$) attained from eq. (3). In This situation, the machine functions as a blocked rotor method. The slip becomes zero if the rotor rotates at the magnetic field speed ($s=0$). The magnetic field speed is expressed at the synchronous speed of DFIG. If the rotor runs higher than the synchronous speed, the slip becomes negative, and the DFIG functions as a generator mode. On the other hand, if the speed of the magnetic field of the stator beats through the intention of the DFIG, it functions as a motor. For that cause, slip defines the functioning of the machine. As a result, the entire parameters of DFIG, moreover, the electrical grid system are known to slip, determining the operation. To ensure the whole analysis is the DFIG, the properties of the generator's rotor necessity are considered. Figure 2,b depicts constant state equivalent network representation, with all parameters referring to the rotor [3]. The method is given by,

$$0 = r'_s \frac{I'_r}{s} + j\omega_r (L'_r + L_M)I'_r + j\omega_r L_M I_s, \quad (6)$$

$$V_r = r_r I_r + j\omega_r (L_r + L_M)I_r - j\omega_e L_M I'_s, \quad (7)$$

where V_r is the rotor voltage. When the rotor is running, the rotor slip is given by

$$S_r = \frac{(\omega_{er} - \omega_r)}{\omega_{er}}, \tag{8}$$

where S_r is the rotor slip.

Equations (6) and (7), the stator with rotor currents phasors in the time domain are obtained by,

$$i_r = |I_r| \cos(\omega_e t + \phi_r), \tag{9}$$

$$i_s = |I_s| \cos(s r \omega_e t + \phi_s - \theta_{eff}), \tag{10}$$

Accordingly, the entire clarification for a DFIG at the basic frequency of the system considering the stator, as well as rotor effects, is given by,

$$I_s = |I_s| \cos(\omega_e t + \phi_s) + |I_r| \cos(s r \omega_e t + \phi_r - \theta_{eff}), \tag{11}$$

$$I_r = |I_r| \cos(\omega_e t + \phi_r) + |I_r| \cos(s \omega_e t + \phi_r - \theta_{eff}). \tag{12}$$

2.2 PWM RECTIFIER WITH PI CONTROLLER

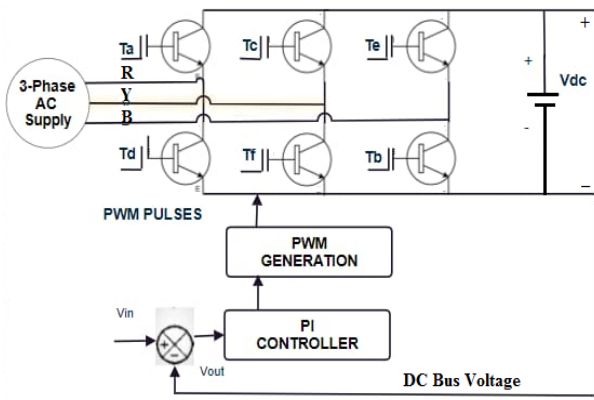


Fig.3 – Rotor side converter.

The 3-phase PWM rectifier converts ac to dc, as shown in Fig. 3. The conventional PWM converter is used for wind systems with permanent magnet alternators. Here, 3-phase ac power received from WECS supported DFIG. The proportional-integral (PI) controller is a feedback controller. It drives the system, which is to be controlled with a weighted total of error and integral value, as shown in Fig. 4. The PI controller is functional to process in current use, from aerospace to motion control, from slow to quick systems. This victory, however, the difficulty of tuning PI controllers has continued lively investigates area. In addition, changes in dynamics system operating points PI controllers must be returned on an accepted basis.

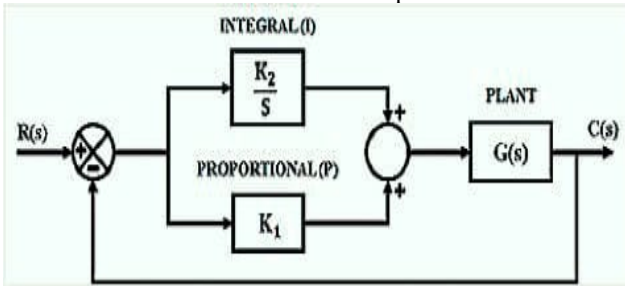


Fig.4 – PI controller.

The PI control system for the manage current i_{dqr} is shown in Fig. 4. The gain k_{p_idqr} is described by,

$$k_{p_idqr} = \frac{\sigma L_r}{\omega_{nr}}. \tag{13}$$

$$k_{i_idqr} = \frac{R_r}{T_{cr}}. \tag{14}$$

where ω_{nr} is the natural angular frequency, $\omega_{nr} = 100/T_{cr}$ and σ is the leakage factor, L_r is the stator-referred rotor inductance, R_r is the stator-referred rotor resistance, T_{cr} is the rotor time constant, and $T_{cr} = \sigma L_r / R_r$.

2.3 THREE-PHASE INVERTER WITH LC FILTER

The inverter converts dc voltage into ac voltage. Three phases voltage source inverter provides three-phase ac voltage as shown in Fig. 5. The voltage management scheme uses phase angle involving inverter output voltage and grid voltage. The current management technique uses the PWM technique to control the real as well as reactive components of the current. LC filter attenuates voltage harmonics produced by three-phase voltage source inverters and, finally, 3-phase transformers matching the grid frequency.

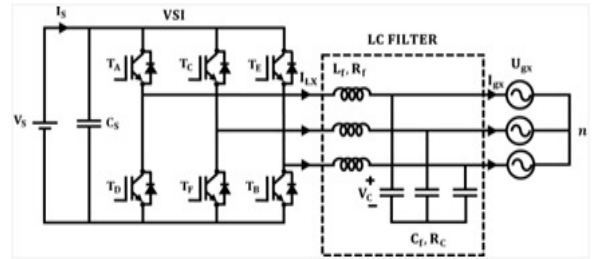


Fig.5 - Grid synchronized 3φ VSI with LC filter.

The values for L and C are calculated from,

$$L = \frac{Z_o}{4\pi f_c}. \tag{15}$$

$$C = \frac{1}{4Z_o \pi f_c}. \tag{16}$$

$$f_c = \frac{1}{4\pi \sqrt{LC}}. \tag{17}$$

where Z_o is the impedance in ohm, C is the capacitance in farad, L is the inductance in henry, and f_c is the cut-off frequency in hertz.

2.4 ANN CONTROLLER AND DQ THEORY BASED GRID SYNCHRONIZATION AND FEEDFORWARD NEURAL NETWORK

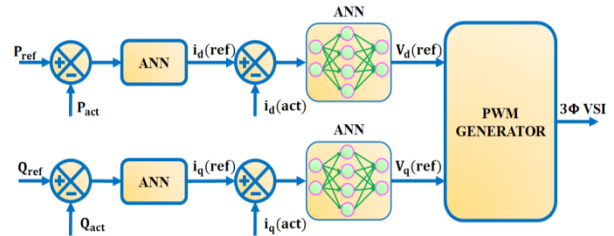


Fig.6- DFIG power control based on ANN Controller.

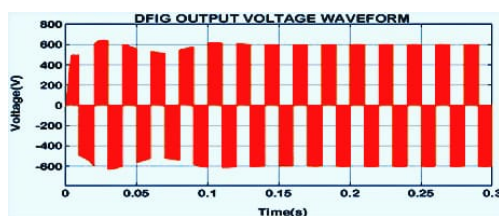
ANN controller, which replicates the workings of the human brain, comprises several interconnected artificial neurons. With the ability to accurately approximate a broad range of nonlinear functions, ANN has recently been used more frequently to identify and manage nonlinear dynamic systems in power electronics. It effectively enhances grid synchronization stability by providing a quicker dynamic response. By comparing actual real power moreover, reactive power obtained from the 3-phase grid with the required set

reference real power during reactive power value of error is fined as shown in Fig. 6. Obtained value of error in totaling to the change of error is specified as an input-to-input layer of ANN system. The obtained error is then processed in a hidden layer based on activation function, bias, and weights.

A synchronous reference framework run, also identified as dq control, is supported by the reference framework transformation element used for transforming current in addition to voltage restrictions of the function grid to reference framework revolving synchronously. Transformation is acquired by Clarke as well as Park transformation techniques, which is converting abc toward $\alpha\beta$ as well as $\alpha\beta$ on the way to dq. Dq power is a new name for synchronized reference framework control. To convert 3-phase time unstable signals keen on dc signals, it alters grid voltage; moreover, current keen on a frame to spins synchronously by way of grid power vector. Making computations considerably simpler is a crucial objective of transforming 3-phases' immediate voltages in addition to currents keen on the synchronously revolving reference work dqo frame. The subsequent benefit is giving the scheme operator autonomous control more than the active (d-axis) and reactive (q-axis) apparatus of currents. The modeling of 3-phase VSI is performed using dq theory, which utilizes direct (D) and quadrature (Q) components. By using the ANN controller, the issue of voltage stability is reduced. Moreover, dc link voltage is maintained without any interruption. Despite variance load, the DSTATCOM model effectively maintains unity power factor and minimum Total harmonics Distortion (THD). The development of data during neurons has improved more than lots of units. When the adaptation in the foundation of output standards is significant since system output is composed of dynamic performance. Based on top features and function demand, convenience is a choice of architectures in neural systems. The arrangement of the neural network must be done using such a technique to facilitate the essential output set formed by the functioning of the set. Setting the weights accurately using earlier accepting is an individual technique. Preparing neural networks near teaches patterns and creating modified weights in unity through several learning rules is a new process, as shown in Fig. 6.

3. SIMULATION AND HARDWARE RESULTS DISCUSSION

3.1 SIMULATION RESULTS OF ANN-BASED CONTROL SCHEME



(a).

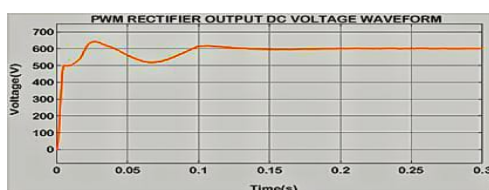
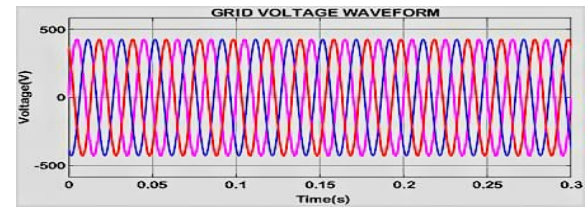


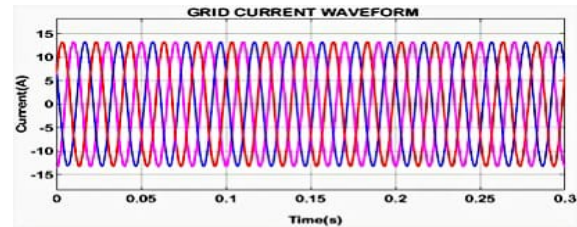
Fig.7 – a) DFIG output voltage; (b) Dc-bus voltage waveform.

The waveforms demonstrating the output voltage of

the DFIG-supported WECS and PWM Rectifier are shown in Fig. 7.



(a)



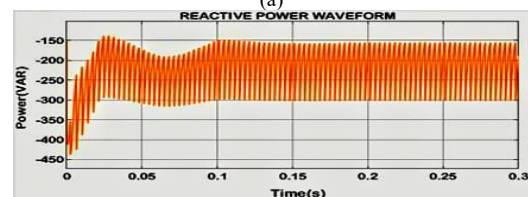
(b)

Fig. 8 – (a) waveforms of 3-phase grid voltage; (b) waveforms of 3-phase grid current.

Due to the irregular character of the wind, the ac output voltage is obtained when DFIG-supported WECS is not constant. At that time, the wind speed was maintained at 15 M/S for the MATLAB simulation. The PWM Rectifier is connected by a DFIG-supported WECS, which eliminates oscillation and converts ac voltage to dc voltage. While the dc-link voltage is sent to 3-phase inverters, it alters dc to ac. Ac voltage obtained is fed to 3-phase grids via a filter to reduce ripples. The valid dq theory supported control used for 3-phase VSI, reducing the process of dq theory current harmonics. The waveforms indicate a 3-phase grid voltage in addition to the current, as shown in Fig. 8. The grid output voltage gained is specified by 400 V, which is normally constant, lacking any fluctuations; the stable grid output voltage and grid output current of 12.3 A.



(a)



(b)

Fig. 9 – 3-phase grid: (a) real power waveform; (b) reactive power waveform.

The waveforms are focused on the magnitude of the real and reactive power of the 3-phase grid, as shown in Fig. 9. The Real power value is 8200 W, and the magnitude of reactive power, which is reasonably less, is about -150 VAR. Figure 10 shows the obtained fraction THD (1.1 %) value to validate the proposed methodology's involvement in the THD minimization method. Reducing reactive power because of additional insignificant effects in the voltage stage retains voltage stability and ensures valuable grid management. DFIG supported WECS

Simulation parameter given in Table. 1.

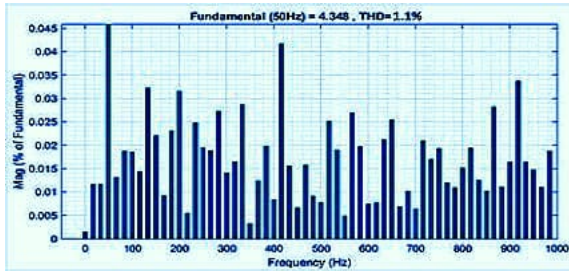


Fig. 10 – THD waveform.

3.2 HARDWARE RESULTS OF ANN-BASED CONTROL SCHEME

Figure 11 shows a hardware snapshot of the proposed system. Ac input power is given to the step-down transformer, which converts 230 V / 12 V and is fed to the PWM rectifier. Subsequently, the PWM rectifier converts the ac supply into a dc supply. The PWM rectifier is controlled using a PI controller-based pulse width modulation technique. The dc output power is directly fed to the dc-link capacitor circuit. Dc link capacitor voltage is a buck-boost fine-tuning function that depends upon the necessary grid power level. The dc voltage is directly fed to the PWM inverter circuit for the inverter converter dc to ac. Moreover, the inverter is controlled by ANN using the PWM technique. The PWM inverter produces square wave output. The square wave output is fed to the LC filter, which filters the harmonic content in the ac output. Finally, pure ac sine wave (40 V) is fed to the grid network system as shown in Fig. 12. Role of the microcontroller, any changes have occurred in grid side voltage. As a result, fine-tuning the pulse driver circuit, without human intervention, changes the pulse width to the grid side converter and the generator side converter. The inverter and rectifier can produce an output voltage that matches the grid voltage based on pulse width.

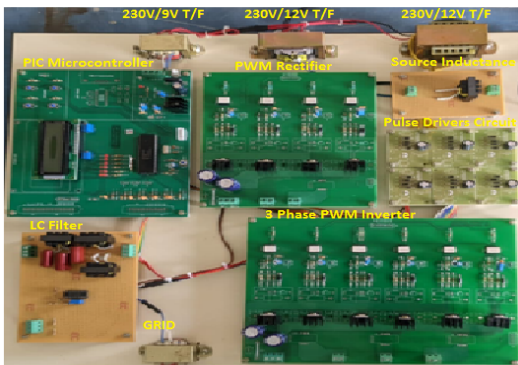


Fig. 11 – Hardware snapshot.

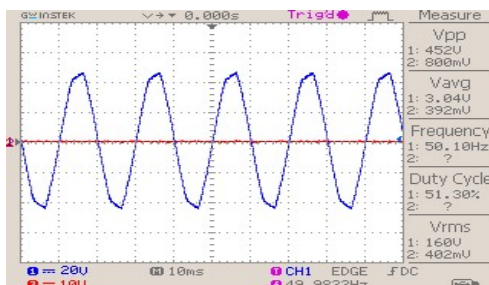


Fig. 12 – Hardware Results using DSO.

4. CONCLUSION

This paper proposes a WECS system for reactive power compensation in the distribution system by utilizing an ANN controller. The proposed method, artificial neural network-based dq theory, extracts reference current from source current for harmonics and reactive power mitigation. The proposed model THD level is 1.1 % (Fig. 10) achieved compared to the exciting model [8–13]. The exciting models are achieved greater than 3 % for THD values using MATLAB Simulink. THD reduction and power quality improvement are the main objects of the proposed model. As a result, overcoming the THD value for the proposed system compared to the exciting system. The simulation outcomes show a highly reasonable state and output evaluation performance. Experimental prototype hardware models are examined, as well as their effectiveness. In future work, the DFIG will be used to improve power quality. Wind power technology and other renewable energy technologies must be introduced in colleges and schools, which may increase its scope. In India, a metro network can be a great source of wind power generation as it will need lighter equipment than conventional wind turbines to connect the wind generated by the commute of metro trains.

APPENDIX

Table 1
Simulation parameters:

S. No	Specifications	Value
1.	Number of wind Turbines and Speed	4.no & 15M/S
2.	DFIG Stator R_s , L_s (p.u)	0.023,0.18
3.	DFIG Rotor R_r' , L_r' (p.u.)	0.016,0.16
4.	DFIG LM, Inertia constant, Friction Factor, Pair of Pole (p.u)	2.9,0.685,0.01,3
5.	PWM Rectifier No., of Bridge arms, R_s , C_s	3,1e5, inf.
6.	3 Phase Inverter	3,1e5, inf.
7.	RL filter R, L	1000 Ω , 10e-(H)
8.	RC Filter R, C	0.5 Ω , 100e-6 (F)
9.	Load (RLC) Vrms, Frequency, Power	440 V, 50Hz, 5000 W

ACKNOWLEDGEMENTS

I would express my sincere gratitude to my beloved Chairman Er. K. Karunanithi, for his kind inspiration and support and for providing the necessary infrastructure to complete this project and research work. I sincerely thank my beloved CEO, Dr. R. Sakthi Krishnan, for his kind stimulation and support. I wish my gratitude to my beloved Principal, Dr. S. Baskaran, for providing us with an opportunity to do the research work. I would like to express my heartfelt thanks and hearty appreciation to my parents Mr. P. Elumalai, Mrs. E. Rukkumani. My beloved wife, Dr. R. Vijaya Lakshmi, B.S.M.S., and My Sweetheart Sons, Mr. R. Renu Prasaath and Mr. R. Sriram, for supporting me regularly. Finally, I would express my sincere gratitude to my friends Mr. K.S. Kavin (ABT), Dr. V. Raji, Mr. V. Suresh, Dr. P. Prabakaran (BIT), Mr. V. Dilip and Mr. B. Anbu Sivam for given regular support to me.

Received on 17 October 2023

REFERENCES

1. T. Jiang, Y. Zhang, *Robust predictive rotor current control of doubly fed induction generator under unbalanced and distorted grid*, IEEE Trans. Energy Convers (2021)
2. D. Xu, F. Blaabjerg, W. Chen, N. Zhu, *Advanced control of doubly fed induction generator for wind power systems*, Hoboken, NJ, USA, Wiley (2018).
3. M.R.A. Kashkooli, S.M. Madani, T.A. Lipo, *Improved direct torque control for a DFIG under symmetrical voltage dip with transient flux damping*, IEEE Trans. Ind. Electron., 67, 1, pp. 28–37 (2020).
4. C. Cheng, H. Nian, *Low-complexity model predictive stator current control of DFIG under harmonic grid voltages*, IEEE Trans. Energy Conv., 32, 3, pp. 1072–1080 (2017).
5. P. Cheng, C. Wu, J. Ma, F. Blaabjerg, *Coordinated derived current control of DFIG's RSC and GSC without PLL under unbalanced grid voltage conditions*, IEEE Access, 8, pp. 64760–64769, (2020).
6. L. Fan, S. Yuvarajan, R. Kavasseri, *Harmonic analysis of a DFIG for a wind energy conversion system*, IEEE Trans. Energy Conv., 25, 1, pp. 181–190 (2010).
7. ***Centre for Wind Energy Technology, Ministry of New and Renewable Energy, Central Government of India, Indian Wind Grid Code, New Delhi, India (2009).
8. S. Tamalouzt, K. Idjdarene, T. Rekioua, R. Abdessemed, *Direct torque control of wind turbine driven doubly fed induction generator*, Rev. Roum. Sci. Techn. – Électrotechn et Énerg., 61, 3, pp. 244–249 (2016).
9. F. Amrane, A. Chaiba, B.E. Babes, S. Mekhilef, *Design implementation of high-performance field-oriented control for grid-connected doubly fed induction generator via hysteresis motor current controller*, Rev. Roum. Sci. Techn. Électrotechn. et Énerg., 61, 4, pp. 319–324, Bucharest (2016).
10. F. Amrane, A. Chaiba, B. Francois, B.E. Babes, *Real time implementation of grid - connection control using robust PLL for WECS in variable speed DFIG-based on HCC*, IEEE Xplore (2017).
11. F. Amrane, A. Chaiba, *A novel direct power control for grid connected doubly fed induction generator based on hybrid artificial intelligent control with space vector modulation*, Rev. Roum. Sci. Techn. -Électrotechn. et Énerg., 61, 3 pp. 263–268 (2016).
12. F. Amrane, A. Chaiba, B. Francois, B.E. Babes, *Experimental design of stand-alone field-oriented control for WECS in variable speed DFIG-based on hysteresis current controller*, IEEE Xplore (2017).
13. B. Babes, A. Boutaghane, N. Hamouda, *Design and real-time implementation of an adaptive fast terminal synergetic controller based on dual BF neural networks of voltage control Dc to Dc step down converter*, Electrical engineering, Springer (2022).
14. M.M. Kiani, W. Wang, W. Lee, *Elimination of system-induced torque pulsations in doubly-fed induction generators via field reconstruction method*, IEEE Trans. Energy Conv., 30, 3, pp. 1228–1236 (2015).
15. J. Samanes, E. Gubia, J. Lopez, R. Taberna, *Sub-synchronous resonance damping control strategy for DFIG wind turbines*, IEEE, 8 (2020).
16. M.A. Soliman, H.M. Hasanien, A. Al-Durra, M. Debouza, *High performance frequency converter-controlled variable-speed wind generator using linear-quadratic regulator controller*, IEEE Transactions on Industry Applications, 56, 5, pp. 5489–5498 (2020).